Atmos. Chem. Phys. Discuss., 1, 193–220, 2001
www.atmos-chem-phys.org/acpd/1/193/

Atmospheric Chemistry and Physics Discussions

Coastal zone production of IO precursors: A 2-dimensional study

L. J. Carpenter[1], K. Hebestreit[2], U. Platt[2], and P. S. Liss[3]

[1]Department of Chemistry, University of York, York, YO10 5DD, U.K.
[2]Institut für Umweltphysik, University of Heidelberg, INF 229, D-69120 Heidelberg, Germany
[3]School of Environmental Sciences, University of East Anglia, Norwich, NR4 7TJ, U.K.

Received: 13 August 2001 – Accepted: 16 August 2001 – Published: 3 September 2001
Correspondence to: L. J. Carpenter (ljc4@york.ac.uk)

Abstract

At Mace Head, Eire, in the coastal East Atlantic, diiodomethane has been identified as an important precursor of iodine oxide radicals. Peak concentrations of both CH_2I_2 and IO at low water indicate that the intertidal region is a strong source of organo-iodines. Atmospheric measurements of CH_2I_2 made in marine air are used in conjunction with a 2-dimensional model incorporating horizontal and vertical dispersion to provide estimates of the intertidal and offshore fluxes of CH_2I_2 upwind of Mace Head. The strong signature of photolysis in the CH_2I_2 observations indicates that the emissions are not entirely local/coastal, but must include an additional offshore source. Good agreement between model and measured CH_2I_2 concentrations is achieved with an offshore flux of 2×10^4 molecules cm^{-2} s^{-1} and an intertidal flux ranging from 1.3×10^9 molecules cm^{-2} s^{-1} (low water) to 6.5×10^8 molecules cm^{-2} s^{-1} (high water), the latter over a 100 m wide coastal belt. The coastal emissions at low water are in good agreement with independent estimates made from seaweed emission data. We estimate that, although intertidal emissions are $\sim$ 4 orders of magnitude higher than those offshore, their contribution to the measured CH_2I_2 concentrations at 10 m height is only $\sim$ 50%.

1. Introduction

The last decade established that catalytic cycles involving halogen oxide radicals (BrO with smaller contributions from IO and ClO) were responsible for rapid ozone depletion events in the Arctic boundary layer during spring (Barrie et al., 1988; Bottenheim et al., 1990; Barrie and Platt, 1997). More recently, the IO radical has been identified in Antarctica (Friess et al., 2001) and in the mid-latitudes (Alicke et al., 1999; Allan et al., 2000) in conjunction with organoiodine precursors (Carpenter et al., 1999), confirming the potential for the more widespread occurrence of boundary layer ozone depletion. Formation of IO is driven by ocean-atmosphere exchange of organo-iodines that are photolysed quickly within the marine boundary layer. Previous studies at Mace Head

ACPD

1, 193–220, 2001

found that a range of photolabile iodine containing organics including CH_3I, C_2H_5I, CH_2ICl, CH_2IBr and CH_2I_2 were present in sufficiently high concentrations to sustain IO levels of a few parts per trillion (ppt), via the following reactions:

$$RI \xrightarrow{h\nu} R + I \quad (1)$$

$$I + O_3 \rightarrow IO + O_2 \quad (2)$$

Of the organoiodines measured, CH_2I_2 was found to be the most important iodine precursor (Carpenter et al., 1999). The photodissociation lifetime of diiodomethane is only a few minutes at midday (Mossinger et al., 1998).

The impact of IO on ozone concentrations depends on the detailed gas phase and heterogeneous chemistry following reaction (2). Computational modelling investigations indicate that the rate of ozone destruction associated with iodine photochemistry in the marine boundary layer could equal that from HO_x photochemistry (Vogt et al., 1999; Stutz et al., 1999; McFiggans et al., 2000). Prediction of the global extent of iodine photochemistry is currently not possible because of the high uncertainty regarding the emissions and distributions of iodine precursors. Shipboard experiments have identified CH_2ICl (Klick and Abrahamsson, 1992; Schall et al., 1997) and CH_2I_2 (Schall et al., 1997) in the open ocean, although it is not yet established whether these originate from microalgae (phytoplankton) or other (e.g. photochemical) sources. That coastal macroalgae are prolific emitters of a wide range of organic halogens is without doubt (e.g. Gschwend et al., 1985; Nightingale et al., 1995; Pedersén et al., 1996; Carpenter et al., 2000 and references therein), although the global budgets of seaweed emissions are very uncertain.

During the ACSOE (Atmospheric Chemistry Studies in the Oceanic Environment) experiment at Mace Head in 1997, macroalgal emissions were observed to have a direct impact on the local atmosphere, as reflected by the peak air concentrations of polyhalogenated halocarbons occurring at low water (Carpenter et al., 1999). These observations may be attributed to direct emission into the surrounding air from exposed macroalgae at low tide and/or increased emissions due to oxidative stress of algae

ACPD
1, 193–220, 2001

upon exposure (Carpenter et al., 2000). At high tide, emissions from submerged beds are diluted in seawater and may undergo photolysis before exchange at the air- sea interface.

Measurements of organo-iodines and IO radicals at Mace Head were repeated during the 1998 EU project PARFORCE (New Particle Formation and Fate in the Coastal Environment). In this study we utilise the dependence of organohalogens and IO concentrations on tidal height to evaluate the relative importance of coastal and offshore emissions of CH_2I_2, providing further information on sources of the IO radical. A Eulerian photochemical box model and a Lagrangian 2-dimensional model are used to estimate coastal and open ocean fluxes of CH_2I_2 and to predict its horizontal and vertical distributions in the coastal region.

2. Experimental

Mace Head is located on the remote western coast of County Galway, Eire (53° 19' N, 9° 54' W). The site is well known for background air measurements and receives relatively clean marine air from the prevailing westerly sector associated with the easterly tracking cyclonic systems of the North Atlantic. The rocky upper littoral zone and cold waters provide favourable conditions for seaweeds.

2.1. Halocarbons

During the period 5–24 September 1998, halocarbons in air were monitored in-situ every 40 minutes with a Hewlett Packard 6890/5973 gas chromatograph/mass spectrometer (GC/MS) system. The GC/MS was operated in a laboratory situated ca. 100 m from the high tide mark, with a sampling inlet located with an open fetch to the ocean at a height of approx. 12m above mean sea level (MSL). The system is developed for automated air sampling and is described fully in Carpenter et al. (1999). Analysis was also performed on discrete samples of surface seawater and the water surrounding in-

ACPD
1, 193–220, 2001

cubated seaweeds. For a full description of analytical procedures for air and seawater analyses during PARFORCE see Carpenter et al. (2000).

2.2. IO measurements by DOAS

Over a 1-month period from 8 September until 8 October 1998 LP DOAS (Long-Path Differential Optical Absorption Spectroscopy (Platt, 1994)) measurements of the halogen oxides IO, OIO and BrO and of other atmospheric trace gases including NO_2, O_3, HCHO, HONO and NO_3 were carried out whenever the visibility allowed reasonable signal to noise ratios.

Briefly, the principle of DOAS is the identification and quantification of atmospheric trace gases by their specific narrow (< 5 nm) band optical absorption structure in the open atmosphere, separating trace gas absorption from broad band molecule and aerosol extinction processes, thus allowing very sensitive detection of many molecular species (see e.g. Platt and Perner, 1983). The identification of the gases is unambiguous since their specific absorption structure is, similar to a fingerprint, unique. Calibration of the instrument is not necessary as long as the absorption cross section is known.

A DOAS instrument based on the principle of Platt and Perner (Platt and Perner, 1983) was used at Mace Head. It incorporates a combination of two coaxially arranged Newtonian telescopes, one collimating the light of a Xe-short-arc lamp through the atmosphere, the second recollecting the beam reflected by an array of quartz prism retroreflectors. The telescopes were set up in a laboratory about 20 meters from the shore, while the retroreflector array was placed on the northern shore of the bay. The light beam was running at an average height of 10 meters above the ocean with a light path length of 2×7.27 km. A 0.5 m Czerny-Turner spectrograph ($f = 6.9$, 600 gr/mm grating, thermostated to 30 ± 0.3°C), in combination with a 1024 pixel photodiode array detector (thermostated to -15 ± 0.3°C), was coupled to the telescope by a quartz fibre, which also performed the task of a mode mixer (Stutz and Platt, 1997). Iodine oxide was measured in the wavelength range from 414 to 437 nm with

ACPD
1, 193–220, 2001

a spectral resolution of about 0.5 nm (a dispersion of 0.078 nm/pixel). Three further wavelength regions were chosen to detect BrO (335 $\pm$ 40 nm) (Hönninger, 1999), OIO (550 $\pm$ 40 nm) (Hebestreit, 2001), NO_3 (645 $\pm$ 40 nm) and the other species absorbing in the respective wavelength regions (O_3, SO_2, NO_4, HCHO, NONO). Besides NO_3, all spectra were recorded using the multi channel scanning technique (Brauers et al., 1995). The concentrations of IO were derived using a least squares fit mixer (Stutz and Platt, 1997) of the reference spectra of H_2O, NO_2 and IO, together with a sixth order polynomial to the atmospheric absorption spectrum. The IO reference spectrum was measured in our laboratory, since no absorption cross section of sufficient resolution was available. NO_2 was measured in a reference cell in the field. Absolute values for both spectra were determined by comparison with literature cross sections (Cox et al., 1999; Harder et al., 1997; Hönninger, 1999). The H_2O reference was calculated by a convolution of the instrument function with the absorption cross section of the HITRAN database (HITRAN, 1987).

2.3. Model description

A 3-day period (18–20 September 1998, Julian days 261–263) of clean marine south-westerly air with stable temperatures (17.2 $\pm$ 1.9°C) and wind speed (5.5 $\pm$ 1.0 m s^{-1}) was selected as a case study for evaluation of marine emissions. Data were evaluated using models written in the FACSIMILE language. The photolysis rate of diiodomethane (J-CH_2I_2) was computed using a 2-stream radiative transfer model (Hough, 1988), with absorption cross-sections from Mossinger et al. (1998) and TOMS O_3 column data (http://toms.gsfc.nasa.gov/ozone/ozone01.html). Photolysis rates were corrected for cloud cover using the ratio of measured/modelled UVA data. The conventional box model assumed a boundary layer height of 1000 m whereas the 2-dimensional model incorporated a 11km long by 1000 m high slice through the atmosphere divided into cells of 100 m length and 10 m height. Both models were driven by 40-minute mean photolysis rates and a coastal CH_2I_2 flux dependent upon 40-minute means of tidal height. In the 2D model, CH_2I_2 was emitted into the bot-

tom cell and transported across consecutive cell faces using the finite volume method to discretise the spatial partial derivatives, given by:

$$\frac{\partial C}{\partial t} = Q + D\frac{\partial^2 C}{\partial x^2} - u\frac{\partial C}{\partial x} \quad (3)$$

where C is the concentration of CH_2I_2, Q is the net rate of production and destruction, D is the diffusion coefficient (set to zero for horizontal transport), the third term representing advection, with u the horizontal wind speed. Horizontal wind speed was parameterised with 40-minute averages of the measured mean values at 3 m height (de Leeuw et al., 2001). Measurements made at 22 m were typically ∼10–15% higher (de Leeuw et al., 2001) as expected from the logarithmic dependence of wind speed with height and a roughness length, z_0, of $\sim 10^{-4}$ m (Kunz et al., 2000). The simplification of assuming a height-independent wind speed should only introduce a significant error (over 20%) at altitudes of over ∼50 m.

The rate of transport across the vertical boundary faces of each cell was described by replacing δx with δy and the eddy diffusivity coefficient, K_z, in place of D. The diffusivity coefficient was assumed to vary with height in the surface layer according to (cf. Stull, 1988):

$$K_z = \frac{\kappa u_* z}{\phi(z/L)} \quad (4)$$

where κ is the von Karman constant (κ = 0.4), z is height, u_* is the friction velocity and $\phi(z/L)$ is a stability correction equal to unity during neutrally stratified boundary layer conditions, which prevailed at Mace Head (de Leeuw et al., 2001). The friction velocity was set to the mean of ∼0.3 m s^{-1} measured during the chosen 3 days of study (de Leeuw et al., 2001).

ACPD
1, 193–220, 2001

3. Results and discussion

3.1. Relationships of iodine species with tidal height and solar radiation

Analysis of PARFORCE data showed that tidal height (TH) and solar radiation (SR) were correlated with CH_2I_2, IO, and to a lesser extent, CH_2IBr air concentrations. Figure 1 shows IO, tidal height and solar radiation at 555 nm (photopic flux in kW/m^2 = klx) for the period 9–15 September. The daily IO maximum shifted simultaneously with the minimum in TH (about one hour from day to day), showing that both solar flux and tidal height controlled the time of the IO peak. It is clear from Fig. 1 that the maximum IO concentrations occurred when the lowest tidal heights overlapped significantly with maximum solar irradiance. Figure 2 shows correlations of IO versus TH for daytime values only **(d)**, all data **(a)**, and night-time values **(n)** of the 4 week measurement period. Under daylight conditions, high IO values were clearly associated with low tidal height, while at night no correlation between IO and TH was found. The correlation was described well by an exponential decrease with rising tide (r^2 = 0.96).

Figure 3 illustrates that the influence of both tidal height and solar flux on CH_2I_2 concentrations was observed during the clean marine south-westerly air period 18–20 September 1998. Hebestreit (2001) analysed the whole 3 week period of halocarbon measurements and found that $[CH_2I_2]_{night} = 0.17 - 0.02[TH]$ and $[CH_2I_2]_{all} = 0.12 - 0.0013[SR]$. Scatter plots for CH_2I_2 and CH_2IBr concentrations with TH and SR for the whole campaign period are shown in Fig. 4. Strong evidence for these organic iodines as important photolytic precursors of IO is evident from their decreasing concentrations with solar flux and, during night-time, maxima at low tide. Note that although peak concentrations of organo-iodines were observed at low water, both CH_2I_2 and CH_2IBr exhibited non-zero concentrations above their detection limits of 0.03 pptv even at high tide, presumably due to offshore (open ocean) sources, as discussed later.

Given that the organoiodine precursors exhibited linear dependencies with TH, the cause of the exponential relationship of IO with TH (Fig. 2) does not appear to be explained by source variations and is possibly attributable to the photochemistry of IO.

ACPD
1, 193–220, 2001

It should also be noted that the IO measurements represent averages over ∼7 km, whereas the organoiodines were measured by point sampling.

3.2. Box model simulations

The photochemical box model was used to test the causality of the observed CH_2I_2 correlations. The model was parameterised with J-CH_2I_2 and tidal height data for the 18–20 September. A TH- dependent emission rate was derived which accurately reflected the observed CH_2I_2 dependencies on TH and SR. The best fit to the data was achieved using an emission rate inversely proportional to TH, as shown (arbitary scale) in Fig. 5. The resulting $[CH_2I_2]_{modelled}$ correlations with TH and SR are shown in Fig. 6. Comparison with Fig. 4 shows that the modelled dependencies were in good agreement with those observed, suggesting that the extent of tidal influence in the flux term was parameterised appropriately and that the correlation of CH_2I_2 with SR observed during PARFORCE was caused solely by photolysis of CH_2I_2.

The CH_2I_2 concentrations predicted by the model also showed generally good agreement with the measurements made during 18–20 September, as shown in Fig. 7. Thus it can be inferred that the estimated TH-dependent flux term was generally applicable, since it had been derived from correlations observed during the whole period of measurements. The tidal influence on CH_2I_2 concentrations at Mace Head was clearly significant. However, the flux derived from the box model can only be regarded as a qualitative indicator of emissions. The small source-sampling distance and short lifetime of CH_2I_2 preclude the quantitative use of a box model, which assumes well-mixed concentrations throughout the boundary layer. A 2-dimensional model incorporating atmospheric dispersion is a more appropriate tool for quantitatively investigating emissions in this case.

ACPD
1, 193–220, 2001

3.3. 2-dimensional model simulations

Before carrying out detailed computations, the sensitivity of the output of the 2-dimensional model to the height of the overall grid and of each cell was determined. Figure 8 compares the CH_2I_2 concentrations predicted at 20 m height using (i) a 1000 m high grid with 20 m high cells, (ii) a 200 m high grid with 20 m high cells and (iii) a 200 m high grid with 5 m high cells. The difference between the first two computations was negligible. The slightly higher concentrations predicted by (iii) can be explained by the difference in resolutions: (i) and (ii) were averages of CH_2I_2 over 20–40 m and therefore lower in concentration than the average of 20–25 m.

The final grid size selected was 11 km by 200 m, with 10 m high and 100 m wide cells. Offshore ocean emissions were represented by the first 1 km of the grid and TH-dependent coastal emissions by the following 100 m belt prior to the station. The organoiodine sampling point of the Mace Head station was represented by the second lowest (10–20 m) cell, at a horizontal distance of 1.1 km from the start of the grid. The effect of marine emissions could therefore be observed over the following 10 km and up to 200 m altitude.

An upper limit to the coastal flux was evaluated from the initial model scenario of no ocean emissions. The TH-dependent emission rate used in this scenario was qualitatively the same as shown in Fig. 5, scaled to provide good agreement with the mean observed CH_2I_2 concentrations. The resulting simulations are compared to the CH_2I_2 observations and box model results in Fig. 9. The tidal-height dependent flux required to match the measurements was 5.4 $\times$ 10^9 molecules cm^{-2} s^{-1} at low water and 2.6 $\times$ 10^9 molecules cm^{-2} s^{-1} at high water.

A clear discrepancy between model and measurements is apparent. The 2-dimensional model showed that the small distance between source and sampling left insufficient time for photolysis to deplete daytime levels of CH_2I_2 to the extent observed. As a sensitivity test, the photolysis rate was increased by a factor of two, but this did not resolve the discrepancy. An alternative flux situation was investigated, wherein the

ACPD
1, 193–220, 2001

offshore region was also a source of CH_2I_2. The average surface seawater concentration of CH_2I_2 between 200 m and 5 km offshore of Mace Head during the PARFORCE campaign was 0.52 $\pm$ 0.26 pmol L^{-1} and the mean seawater temperature was 12°C (Carpenter et al., 2000). The equilibrium air concentration at this temperature calculated using the Henry's law coefficient for CH_2I_2 reported by Moore et al. (1995) is 0.1 pptv. Thus, it is difficult to assess whether or not the offshore waters of Mace Head were a source of CH_2I_2 or simply in equilibrium. An upper limit to the flux can however be calculated using a CH_2I_2 concentration in air of zero. From the Liss-Merlivat expression (Liss and Merlivat, 1986) with a square root molecular weight correction for the transfer velocity (Liss and Slater, 1974) and the mean wind speed, an upper limit to the ocean flux was estimated as 2×10^5 molecules cm^{-2} s^{-1}.

Various combinations of coastal and open ocean fluxes within the upper limit of the offshore flux described above were computed. The best fit to the observed CH_2I_2 data was achieved using an ocean flux of 2×10^4 molecules cm^{-2} s^{-1} and a TH-dependent coastal flux of 1.3×10^9 molecules cm^{-2} s^{-1} at low water and 6.5×10^8 molecules cm^{-2} s^{-1} at high water. The coastal flux and a comparison of the 2D simulation (calculated using 40-minute average wind speed data) with observed and box model data are shown in Fig. 10. The figure shows that the 2D model correctly reproduced the daytime depletion of CH_2I_2 when an offshore ocean source was included. The contributions of the offshore and coastal emissions to the modelled CH_2I_2 concentrations at the Mace Head station were found to be approximately equal, due to the larger ocean surface area. A sensitivity study was carried out to test the effect of changing the coastal flux. Doubling the coastal flux increased the modelled CH_2I_2 concentration by a factor of $\sim$four, whereas decreasing the flux by a factor of ten decreased the CH_2I_2 concentration by only a factor of two. Thus, the coastal flux derived should therefore be regarded as an upper limit.

ACPD
1, 193–220, 2001

3.4. Independent estimates of intertidal CH_2I_2 emissions

In addition to atmospheric measurements made during PARFORCE, the release rates of organic bromines and iodines from seaweeds were determined from incubations in seawater of ten species of brown, red and green macroalgae collected in the intertidal or subtidal zones of the rocky shore (Carpenter et al., 2000). These studies provide independent estimates of coastal CH_2I_2 emissions. The most prevalent seaweeds present in the intertidal zone at Mace Head, in common with most Northern European rocky shores (Michanek, 1975), were the brown algae *Laminaria digitata*, *Laminaria saccharina* and *Ascophyllum nodosum*. These algae are also among the most productive in terms of CH_2I_2 emissions, with mean production rates of 8.3, 1.9 and 0.36 pmol g^{-1} fresh weight hr^{-1}, respectively (Carpenter et al., 2000). Estimates of total kelp density from data provided by the Irish Seaweed Industry Organisation (ISIO) are 11.6 kg m^{-2} (Carpenter et al., 2000). However this value includes *Laminaria hyboborea*, which is only present at depth, therefore the kelp density of the intertidal zone should be reduced by ∼25% (Carpenter et al., 2000). Assuming the density is evenly spread between *L.digitata*, *L. saccharina* and *A. nodosum* and over the intertidal zone leads to a total CH_2I_2 emission rate of $\sim 1.5 \times 10^9$ molecules cm^{-2} s^{-1}. Given the many assumptions made in both this estimate and the 2D model estimate of emissions at low water, the remarkable agreement between the two may be fortuitous. However, it demonstrates that our estimate should certainly be of the right order of magnitude. In addition, the agreement suggests that algae emit CH_2I_2 directly into the surrounding air at a similar rate as into a seawater medium (from which the production rates were measured).

3.5. Prediction of spatial variation of CH_2I_2 concentrations

The estimated open ocean and coastal emissions were used in the 2D model to predict the horizontal and vertical distributions of CH_2I_2 in the coastal region. Figure 11 shows that night- time CH_2I_2 concentrations of over 2×10^6 molecules cm^{-3} (0.08 pptv at

ACPD
1, 193–220, 2001

STP) were predicted to be present at altitudes of ∼100 m, several kilometres from the station. However, the uplift of the plume may have been overestimated at night, due to the model utilising 24 h average eddy diffusivity coefficients. During the day, concentrations of over 2 × 10^6 molecules cm^{-3} CH_2I_2 were predicted to be present only near ground level and within ∼100 m of the station horizontally. The modelled variation of CH_2I_2 concentration with time up to 50 m altitude at the horizontal point of the station is shown in Fig. 12.

4. Summary and conclusions

Strong evidence for the organoiodines CH_2I_2 and CH_2IBr as photolytic precursors to the IO radical at Mace Head was shown from the dependence of all three species on tidal height. Iodine oxide concentrations peaked at low water during midday hours and the reactive organoiodines, whose lifetimes are less than 1 hour at midday, peaked when low water coincided with night. Using a 2-dimensional model to simulate atmospheric dispersion, upper limits of the flux rate of CH_2I_2 from exposed seaweed beds at low water at Mace Head was estimated as 1.3 × 10^9 molecules cm^{-2} s^{-1}, and about half this value at high water. The coastal emissions at low water were in good agreement with independent estimates made from seaweed emission and density data. Combined with an offshore emission rate of 2 × 10^4 molecules cm^{-2} s^{-1}, the modelled CH_2I_2 concentrations showed good agreement with the measurements. The model showed that the non- zero CH_2I_2 concentrations observed at Mace Head during the day could be explained by proximity to source. However, some contribution from offshore sources was necessary to reproduce the observed daytime depletion of CH_2I_2, suggesting an (unknown) ocean source of CH_2I_2.

Acknowledgements. We are grateful to Gerrit de Leeuw for supplying micro-meteorological data from PARFORCE, and to Jochen Stutz and Gerd Hönninger for their help performing the DOAS measurements and the evaluation of the DOAS data. We would also like to acknowledge Colin O'Dowd, Gerry Spain and Mick Geever for their organization of the PARFORCE

campaign. Financial support for this project was provided by the Natural Environment Research Council (NERC) grant GR9/03597.

References

Alicke B., Hebestreit, K., Stutz, J., and Platt, U., Iodine oxide in the marine boundary layer, Nature, 397, 572–573, 1999.

Allan B. J., McFiggans, G., Plane, J. M. C., and Coe, H., Observations of iodine monoxide in the remote marine boundary layer, J. Geophys. Res., 105, 14363–14369, 2000.

Barrie, L. A., Bottenheim, J. W., Schnell, R. C., Crutzen P. J., and Rasmussen, R. A., Ozone destruction and photochemical reactions at polar sunrise in the lower Arctic atmosphere, Nature, 334, 138–141, 1988.

Barrie, L.A. and Platt, U., Arctic tropospheric chemistry: an overview, Tellus, 49B (5), 450–454, 1997.

Bottenheim, J. W., Barrie, L. A., Atlas, E., Heidt, L. E., Niki, H., Rasmussen, R. A., and Shepson, P. B., Depletion of lower tropospheric ozone during Arctic spring: The Polar Sunrise Experiment, J. Geophys. Res., 95, 18555–18568, 1990.

Brauers, T., Hausmann, M., Brandenburger, U., and Dorn, H.-P., Improvement of Differential Optical Absorption Spectroscopy with a multichannel scanning technique, Applied Optics, 34, 4472–4479, 1995.

Cox, R. A., Bloss, W. J., Jones, R. L., and Rowley, D. M., OIO and the Atmospheric Cycle of Iodine, Geophysical Research Letters, 26 (13), 1857–1860, 1999.

Carpenter, L. J. and Liss, P. S., On temperate sources of bromoform and other reactive organic bromine gases, J. Geophys. Res., 105, 20, 539–20, 548, 2000.

Carpenter, L. J., Sturges, W. T., Liss, P. S., Penkett, S. A., Alicke B., Hebestreit, K., and Platt, U., Short lived alkyl-iodides and bromides at Mace Head: Links to macroalgal emission and halogen oxide formation, J. Geophys. Res, 104, 1679, 1999.

Carpenter, L. J., Malin, G., Kuepper, F., and Liss, P. S., Novel biogenic iodine-containing trihalomethanes and other short-lived halocarbons in the coastal East Atlantic, Global Biogeochem. Cycles, 14, 1191–1204, 2000.

De Leeuw, G., Kunz, G. J., and O'Dowd, C. D., Micro-meteorological measurements at the Mace Head mid-latitude coastal station, Submitted to J. Geophys. Res., 2001.

Friess, U., Wagner, T., Pundt, I., Pfeilsticker, K., and Platt, U., Spectroscopic Measurements of Tropospheric Iodine Oxide at Neumayer Station, Antarctica, Geophysical Research Letters, 28, 10, 1941–1944, 2001.

Gschwend, P. M., Macfarlane J. K., and Newman, K. A., Volatile halogenated organic-compounds released to seawater from temperate marine macroalgae, Science, 227, 1033–1035, 1985.

Harder, J. W., Brault, J. W., Johnston, P. V., and Mount, G. H., Temperature dependent NO_2 cross sections at high spectral resolution, J. Geophys. Res., 102, 3861–3879, 1997.

HITRAN, HITRAN database 1986 edition, Applied Optics, 26, 4058–4097, 1987.

Hönninger, G., Referenzspektren reaktiver Halogenverbindungen für DOAS Messungen, Diploma thesis, Ruprecht Karls Universität Heidelberg, Heidelberg, 1999.

Hough, A. M., The calculation of photolysis rates for use in global troposheric modelling studies, AERE Report R-13259, 53, HMSO, London, 1988.

Klick, S. and Abrahamsson, K., Biogenic volatile iodated hydrocarbons in the ocean, J. Geophys. Res., 97, 12683–12687, 1992.

Kunz, G. J., Cohen, L. H., and de Leeuw, G., Lidar and micrometeorological measurements during the PARFORCE experiments at the Mace Head Atmospheric Research Station, Carna, Ireland, during September and June 1998.

Liss, P. S. and Merlivat, L., Air-sea exchange rates: Introduction and synthesis, in Role of Air-Sea Exchange in Geochemical Cycling, edited by P. Buat-Ménard, 113–127, D. Reidel Publishing Company, Dordrecht, 1986.

Liss, P. S. and Slater, P. G., Flux of gases across the air-sea interface, Nature, 247, 181–184, 1974.

McFiggans, G., Allan, B., Coe, H., Plane, J. M. C., Carpenter, L. J., and O'Dowd, C., Observations of IO and a modelling study of iodine chemistry in the marine boundary layer, J. Geophys. Res., 105, 14, 371–14, 385, 2000.

Michanek, G., Seaweed resources of the ocean, FAO Fish. Tech. Pap., 138, 127, 1975.

Moore, R. M., Geen, C. E., and Tait, V. K., Determination of Henry's Law constants for a suite of naturally occurring halogenated methanes in seawater, Chemosphere, 30, 1183–1191, 1995.

Mossinger, J., Shallcross, D. E., and Cox, R. A., UV-visible absorption cross-sections and atmospheric lifetimes of CH_2Br_2, CH_2I_2, and CH_2BrI, J. Chem. Soc. Far., 10, 1391–1396, 1998.

Nightingale P. D., Malin, G., and Liss, P. S., Production of chloroform and other low-molecular-weight halocarbons by some species of macroalgae, Limnol. Oceaongr., 40, 680–689, 1995.

Pedersén, M., Collén, J., Abrahamsson, K., and Ekdahl, A., Production of halocarbons from seaweeds–an oxidative stress reaction, Scientia Marina, 60, 257–263, 1996.

Platt, U., Differential optical absorption spectroscopy (DOAS), Chemical Analysis Series, 127, 1994.

Platt, U. and Perner, D., Measurements of atmospheric trace gases by long path differential UV/visible absorption spectroscopy, in Optical and Laser Remote Sensing, edited by Killinger, D. A. and Mooradien, A., 95–105, Springer Verlag, New York, 1983.

Schall, C., Heumann, K. G., and Kirst, G. O., Biogenic volatile organoiodine and organobromine hydrocarbons in the Atlantic Ocean from 42 degrees N to 72 degrees S, Fres. J. Anal. Chem., 359, 298–305, 1997.

Stull, R. B., An introduction to boundary layer meteorology, Kluwer Academic Publishers, Dordrecht, 1988.

Stutz, J. and Platt, U., Improving long-path differential optical absorption spectroscopy with a quartz-fiber mode mixer, Applied Optics, 36, 1105–1115, 1997.

Stutz, J., Hebestreit, K., Alicke, B., and Platt, U., Chemistry of halogen oxides in the troposphere: comparison of model calculations with recent field data, Journal of Atmospheric Chemistry, 34, 65–85, 1999.

Vogt, R., Sander, R., von Glasow, R., and Crutzen, P. J., Iodine chemistry and its role in halogen activation and ozone loss in the marine boundary layer: A model study, J. Atmos. Chem., 32, 375–395, 1999.

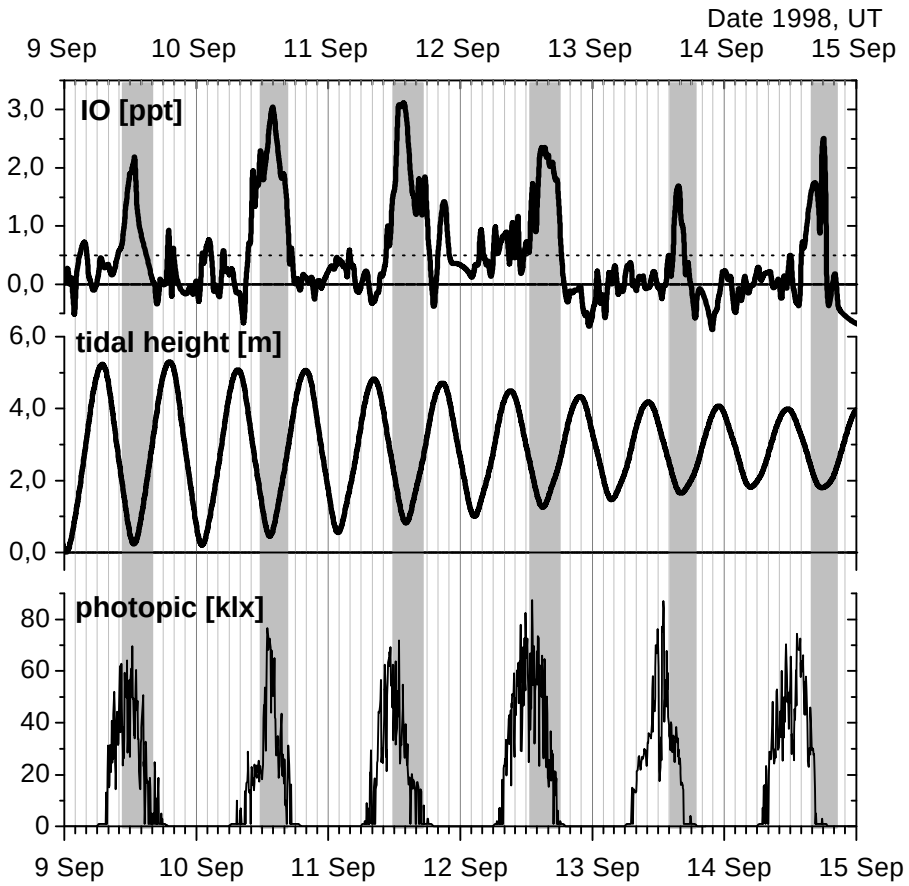

Fig. 1. IO, tidal height and solar radiation during 9–15 September, 1998. The dotted line on the IO graph represents the average detection limit. The grey areas mark the low tide periods.

ACPD
1, 193–220, 2001

Coastal zone production of IO precursors

L. J. Carpenter et al.

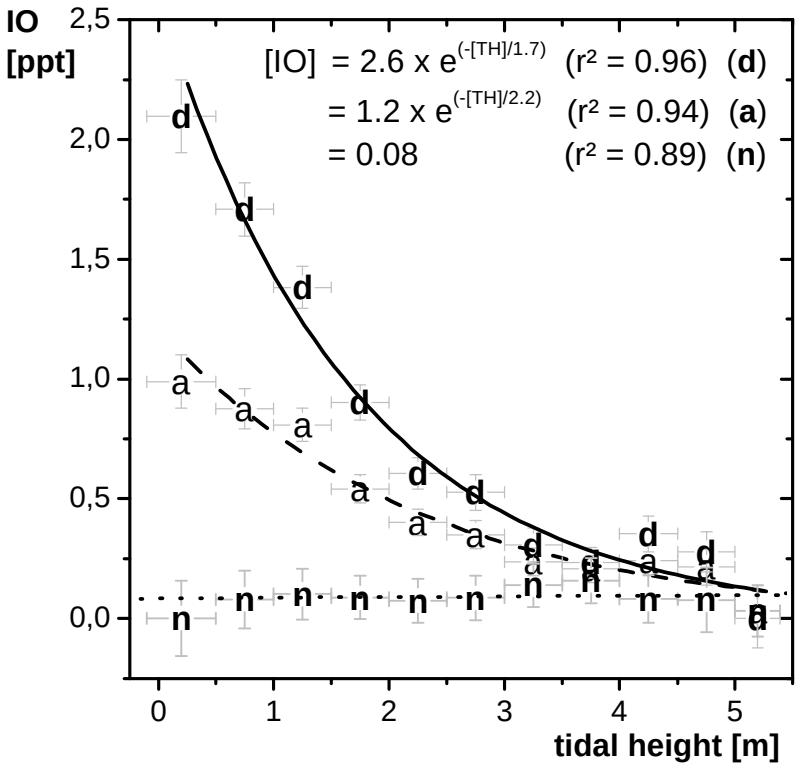

n = night
d = day
a = all data

Fig. 2. Correlation of IO and tidal height during PARFORCE.

ACPD
1, 193–220, 2001

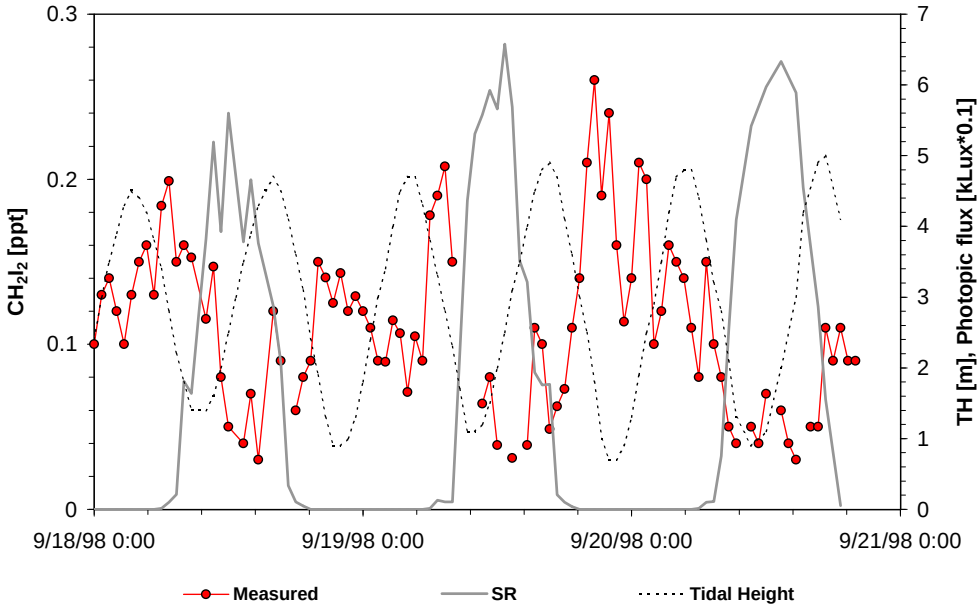

Fig. 3. CH_2I_2, tidal height and solar flux during clean marine conditions.

ACPD
1, 193–220, 2001

Coastal zone production of IO precursors

L. J. Carpenter et al.

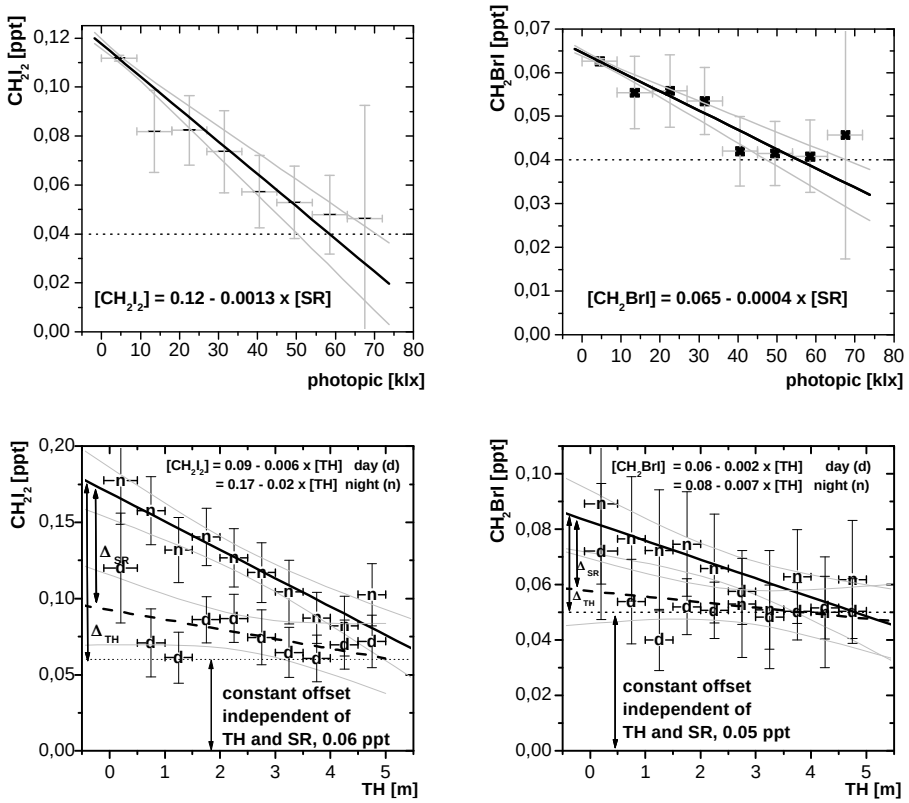

Fig. 4. Correlations of CH_2I_2 and CH_2IBr with SR and TH for the whole measurement period. The correlation with TH is divided into night-time **(n)** and day-time **(d)** values of CH_2I_2 and CH_2IBr, respectively.

ACPD
1, 193–220, 2001

Coastal zone production of IO precursors

L. J. Carpenter et al.

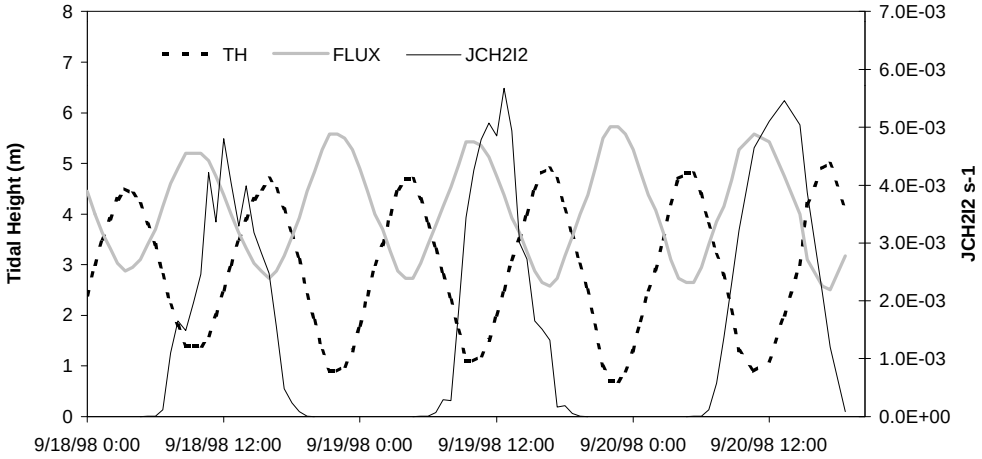

Fig. 5. The tidal-height dependent CH_2I_2 flux rate (FLUX, arbitary units) used in the model, shown with tidal height and J CH_2I_2.

ACPD

1, 193–220, 2001

Coastal zone production of IO precursors

L. J. Carpenter et al.

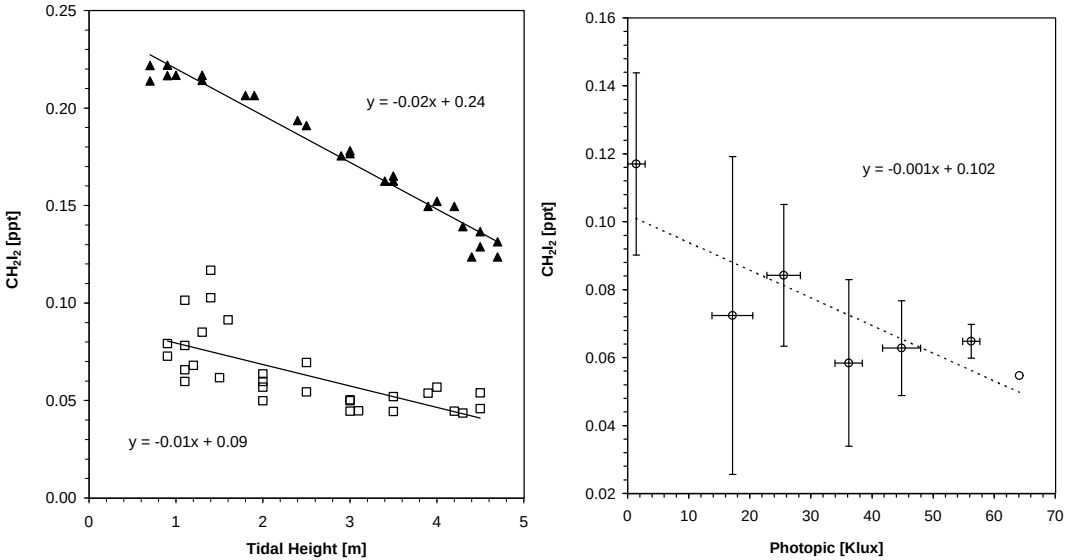

Fig. 6. Correlations of **(a)** tidal height and **(b)** solar flux with CH_2I_2 concentrations predicted by the box model. In Fig. 6a, night-time data is represented by the filled triangles and daytime data by the open squares.

ACPD
1, 193–220, 2001

Coastal zone production of IO precursors

L. J. Carpenter et al.

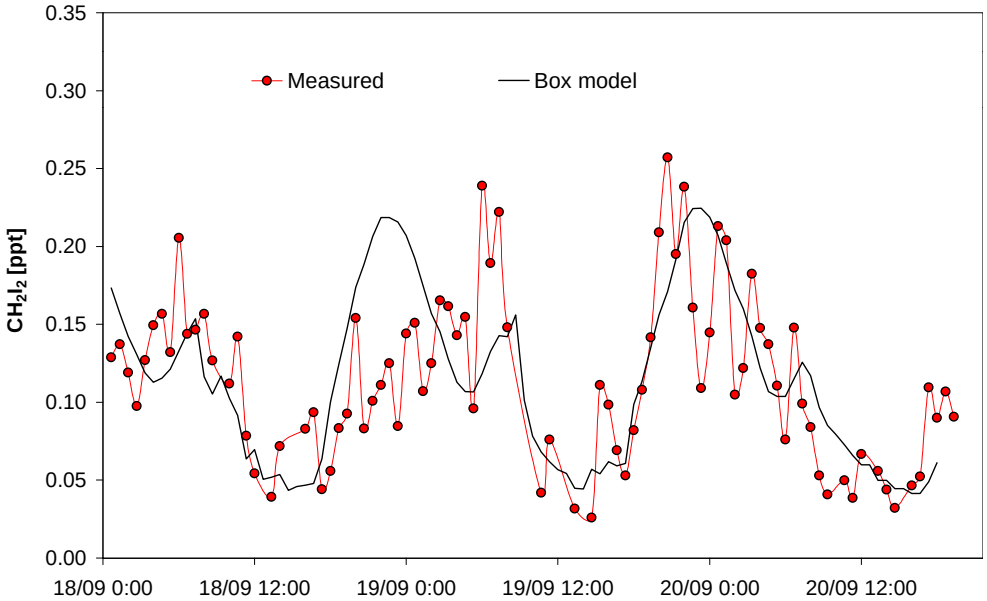

Fig. 7. Comparison of measured and modelled CH_2I_2 concentrations.

ACPD

1, 193–220, 2001

Coastal zone production of IO precursors

L. J. Carpenter et al.

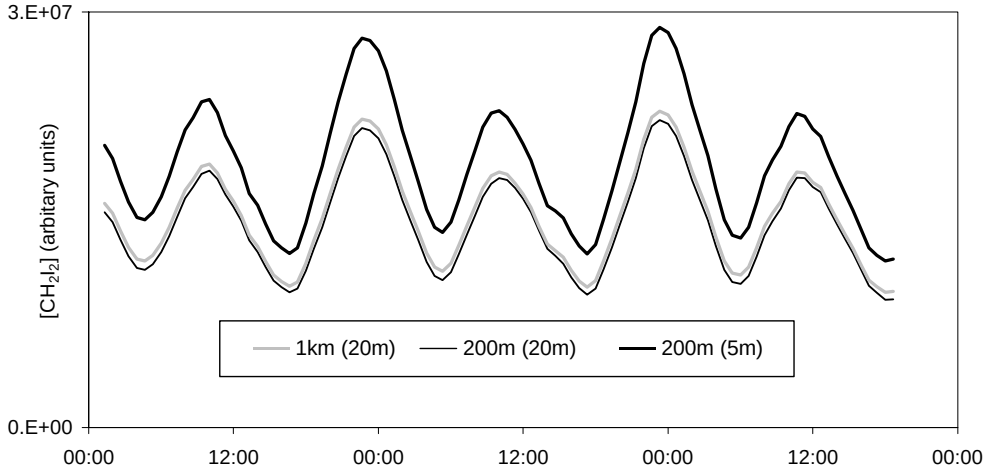

Fig. 8. CH_2I_2 concentrations predicted at 20 m by the 2-dimensional model at different grid heights (1 km and 200 m) and resolutions (20 m and 5 m).

ACPD
1, 193–220, 2001

Coastal zone production of IO precursors

L. J. Carpenter et al.

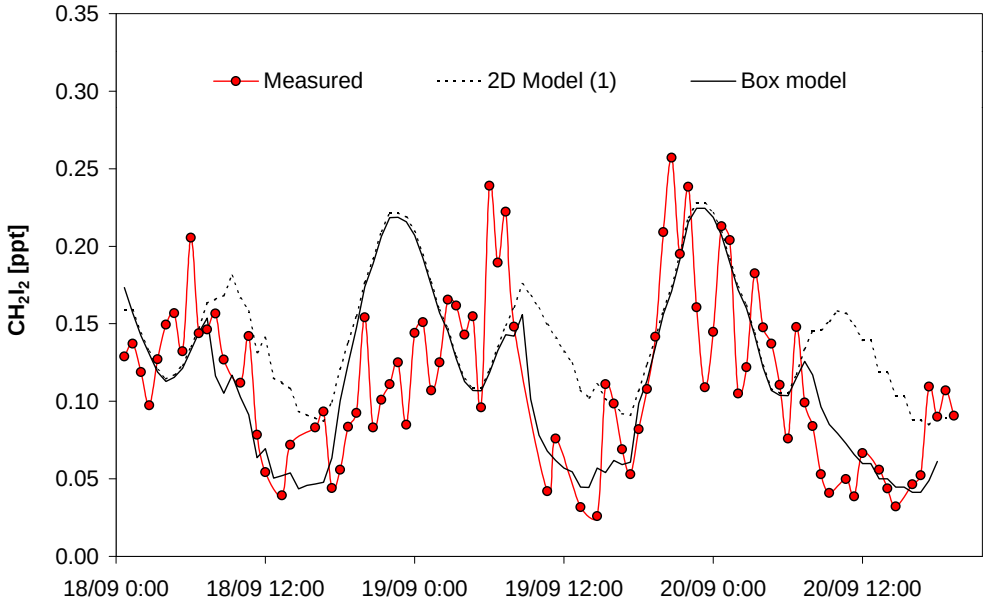

Fig. 9. Comparison of 2D model predictions of CH_2I_2, calculated using only coastal sources, with measurements and box model results.

ACPD
1, 193–220, 2001

Coastal zone production of IO precursors

L. J. Carpenter et al.

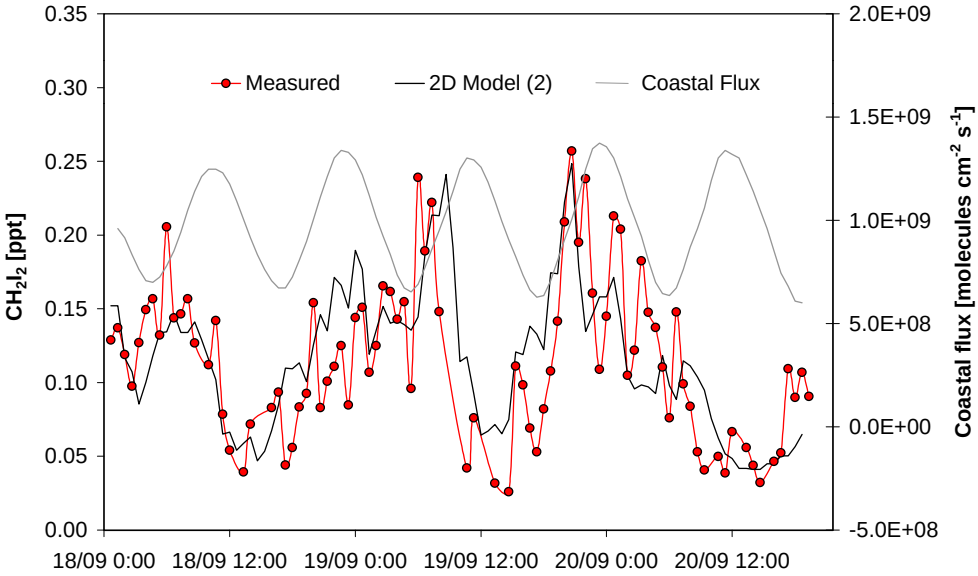

Fig. 10. Comparison of 2D model predictions of CH_2I_2, calculated using both coastal and offshore sources, with measurements. The tidal height – dependent coastal flux inferred by the model is also shown.

ACPD

1, 193–220, 2001

Coastal zone production of IO precursors

L. J. Carpenter et al.

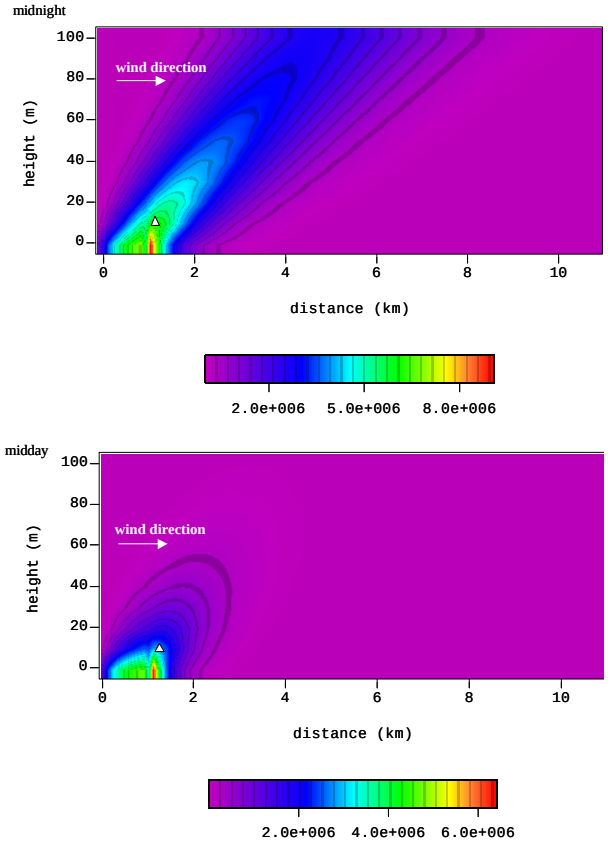

Fig. 11. The spatial variation of CH_2I_2 concentrations predicted by the 2D model at **(a)** midnight and **(b)** midday. The colour scales represent CH_2I_2 concentrations in molecules cm^{-3}. The Mace Head station is represented by the white triangle. On the horizontal axis, the first 1 km is the ocean surface, the next 100 m is intertidal, and the following 10 km represents land.

ACPD
1, 193–220, 2001

Coastal zone production of IO precursors

L. J. Carpenter et al.

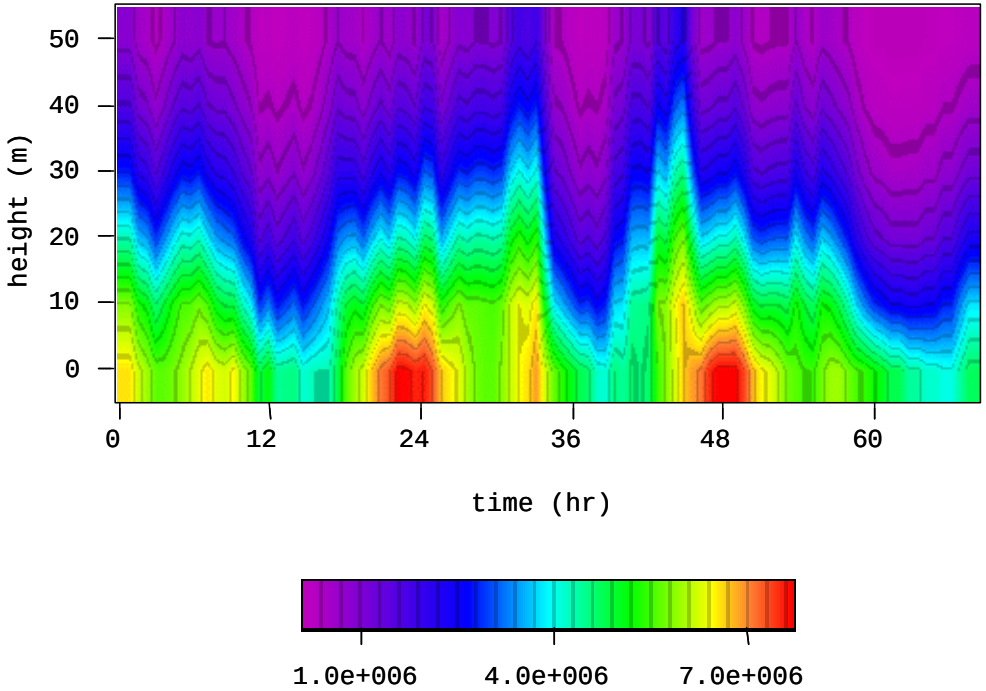

Fig. 12. Variation of CH_2I_2 with height at the Mace Head station as predicted by the 2D model for the period 18–20 September. The colour scale represents the CH_2I_2 concentration in molecules cm^{-3}.

ACPD
1, 193–220, 2001

Coastal zone production of IO precursors

L. J. Carpenter et al.